https://doi.org/10.5194/essd-2026-253
Preprint. Discussion started: 20 April 2026

Open Access Earth System Science Data Discussions

Circum-Arctic Sediment PROvenance Database (CASPROD): A database of mineralogy and geochemistry for the Circum-Arctic surface sediments

Zhengquan Yao[1,2*], Han Feng[1], Ruediger Stein[3,4,5], Yanguang Liu[1,2], Xuefa Shi[1,2], YuriVasilenko[6], Seung-Il Nam[7], Linsen Dong[1,2], Fengdeng Shi[1,2], Kunshan Wang[1,2], Zhihua Chen[1,2], Shuqing Qiao[1,2], Qiuling Li[1], Song Zhao[1], Xinyue Pei[1], Huiyu Guo[1], Yaru Liu[1]

[1] Key Laboratory of Marine Geology and Metallogeny, First Institute of Oceanography, Ministry of Natural Resources, 266061 Qingdao, China

[2] Laboratory for Marine Geology, Qingdao Marine Science and Technology Center, 266237 Qingdao, China

[3] Faculty of Geosciences, University of Bremen, 28359 Bremen, Germany

[4] Frontiers Science Center for Deep Ocean Multispheres and Earth System, Key Laboratory of Marine Chemistry Theory and Technology, Ocean University of China, 266100 Qingdao, China

[5] Alfred Wegener Institute, Helmholtz Centre for Polar and Marine Research, 27568 Bremerhaven, Germany

[6] V.I.Il'Ichev Pacific Oceanological Institute, Far East Branch of the Russian Academy of Sciences, 690041 Vladivostok, Russia

[7] Division of Glacial Environment Research, Korea Polar Research Institute, 21990 Incheon, Korea

***Correspondence:** Zhengquan Yao (yaozq@fio.org.cn)

Abstract

Arctic amplification is fundamentally reshaping the cryosphere, leading to accelerated sea-ice retreat, permafrost thaw, and intensified riverine discharge. These shifts collectively modify sediment source-to-sink dynamic processes in the Arctic Ocean. While surface sediments in this semi-enclosed basin integrate complex signals

https://doi.org/10.5194/essd-2026-253
Preprint. Discussion started: 20 April 2026

Open Access Earth System Science Data Discussions

from diverse Eurasian and North American source regions, disentangling these provenance signatures requires a robust, multi-proxy framework that has historically been hampered by fragmented, heterogeneous datasets. Here, we present CASPROD (Circum-Arctic Sediment PROvenance Database), a standardized and high-resolution mineralogical and geochemical synthesis of Arctic surface sediments. The dataset integrates multi-proxy records from a broad spatial network, comprising 4308 sampling stations, including bulk sediment Sr-Nd isotopes (n=175 stations), detrital zircon U-Pb ages (n=4671 grains from 21 key stations), clay mineral assemblages (n=1647 stations), and detrital mineral proportions (n=2465 stations). These integrated proxies provide cross-validated sediment provenance constraints: Sr-Nd isotopes discriminate between ancient cratonic shields and juvenile orogenic belts; detrital zircon geochronology yields diagnostic age spectra distinguishing Eurasian versus North American crustal affinities; and clay and detrital mineralogy reflects different circum-Arctic sediment provenances, lithologies and transport processes. By synthesizing these diverse datasets, CASPROD delineates robust pan-Arctic spatial provenance domains and transport pathways. This database thus provides a critical benchmark for reconstructing palaeoceanographic, glacial, and sedimentary dynamics over geological timescales. CASPROD is freely available online (https://doi.org/10.6084/m9.figshare.31926927; Yao et al., 2026) in multiple machine-readable formats (e.g., tabular tables, GIS shapefiles, and GEOTIFF).

1. Introduction

The Arctic region is currently warming at a rate approximately four times faster than the global average, a phenomenon known as Arctic amplification (Serreze and Barry, 2011; Rantanen et al., 2022). This rapid warming has accelerated a cascade of environmental responses, including sea-ice attrition and Greenland ice-sheet mass loss, enhanced permafrost thaw, and increased riverine discharge to the Arctic Ocean (White et al., 2007; The IMBIE, 2020; Stroeve and Notz, 2018; Natali et al., 2021). Beyond regional impacts on polar regions, these changes exert far-reaching influences on global climate system through atmospheric and oceanic teleconnections (Screen and Simmonds, 2010; Cohen et al., 2014; Henderson et al., 2021).

Crucially, climate-driven environmental changes have fundamentally reorganized

https://doi.org/10.5194/essd-2026-253
Preprint. Discussion started: 20 April 2026

Open Access Earth System Science Data Discussions

sediment source-to-sink processes in the Arctic Ocean. Sea-ice retreat enhances the efficiency and spatial reach of ice-rafted sediment transport across Arctic basins (Darby, 2003; Eicken et al., 2005; Stein, 2008), while intensified precipitation and permafrost degradation due to thermokarst processes increase the fluvial flux of terrigenous materials (Holmes et al., 2002; Rusakov et al., 2025). In addition, the major circulation systems, including the Beaufort Gyre and the Transpolar Drift (Timmermans and Marshall, 2020), constantly modifies sediment dispersal pathways and redistribution patterns. Consequently, surface sediments act as a valuable archive, preserving integrated signals of sediment provenance, river input, sea-ice rafting, coastal erosion, and hydrodynamical conditions (for review see Stein, 2008).

Sediment inputs to the Arctic Ocean therefore form a complex spatial mosaic derived from geologically diverse circum-Arctic source regions, including the Eurasia, North America, Greenland, and the Canadian Arctic Archipelago (Gordeev, 2006; Martinez et al., 2009). While fluvial systems and coastal erosion supply primary materials, ice-rafted debris (IRD) and ocean currents facilitate basin-wide redistribution of sediments (Darby, 2003; Phillips and Grantz, 2001; McCave and Andrews, 2019). Accurate characterization of modern sediment provenance is thus a fundamental prerequisite for reconstructing paleoenvironmental history, including past source-to-sink process, ice-sheet dynamics, sea-ice history, and paleo-circulation patterns (e.g., Vogt, 1997; Philips and Grantz, 2001; Stein, 2008; Stein et al., 2010, 2025).

A range of provenance tracers, such as Sr-Nd isotopes, clay mineral assemblages, detrital mineral compositions, and detrital zircon U-Pb ages, provide complementary constraints on sediment sources in the Arctic Ocean. Sr-Nd isotopes effectively distinguish sediments derived from juvenile orogenic belts and ancient Archean-Proterozoic cratons (Bazhenova et al., 2017; Maccali et al., 2018; Li et al., 2023), whereas detrital zircon U-Pb age spectra offer robust geochronological fingerprints that discriminate between North American and Eurasian basement affinities (Fedo et al., 2003; Feng et al., 2025). Clay mineral assemblages may reflect source-rock provenance, transport process of fine-grained sediments, and past varying climatic regimes and weathering intensity (e.g., Naidu and Mowatt, 1983; Stein et al., 1994; Wahsner et al., 1999; Thiry, 2000; Viscosi-Shirley et al., 2003; Vogt and Knies, 2009; Saukel et al., 2010; Jang et al., 2023), while detrital mineral assemblages capture coarse-grained signals representative of proximal lithologies (e.g., Vogt, 1996, 1997; Behrends, 1999; Stein, 2008; Wang et al., 2022).

https://doi.org/10.5194/essd-2026-253
Preprint. Discussion started: 20 April 2026

Open Access Earth System Science Data Discussions

Previous efforts have established several foundational databases for specific provenance proxies across the Arctic region. In a comprehensive synthesis study, Stein (2008) systematically compiled and mapped the spatial distributions of clay and detrital minerals throughout the Arctic Ocean, providing a critical reference framework (for data download and complete list of reference see Stein, 2026a, 2026b). This work characterized the composition of clay minerals (i.e., illite, chlorite, kaolinite and smectite) and selected detrital mineral assemblages and highlighted their significance for tracing sediment source regions and transport mechanisms of terrigenous materials (Stein, 2008). The mineralogical dataset was subsequently expanded in more recent compilations, notably by Myers and Darby (2022). In parallel, Maccali et al. (2018) synthesized a comprehensive Sr-Nd isotopic database for Arctic sediments. Despite these important contributions, a comprehensive and integrated provenance database that combines multiple proxies and incorporates newly published data remains lacking.

Here, we address this gap by compiling data from recent literature, with particular emphasis on newly generated datasets obtained from China-Russian joint investigations across the East Siberian Arctic shelf. The dataset integrates newly published Sr-Nd isotopic data (e.g., Li et al., 2023), clay mineral assemblages (e.g., Shi et al., 2018; Li et al., 2021; Jang et al., 2023), and detrital mineral compositions (e.g., Bazhenova, 2012; Dong et al., 2014; Gamboa et al., 2017; Andrews, 2019; Wang et al., 2024). In addition, the compilation is further expanded to include detrital zircon U-Pb geochronology data (Safonova et al., 2010; Wang et al., 2011; Feng et al., 2025). The database is designed with a structure that allows for continual updates, ensuring its long-term utility as a living resource for Arctic provenance research. Integrated analysis of these multi-proxy datasets enables the delineation of pan-Arctic spatial provenance patterns and provides new insights to the key processes governing modern source-to-sink pathways. Moreover, this database serves as a valuable benchmark for reconstructing sedimentary processes, glacial dynamics, and ocean circulation over geological time.

2. The CASPROD dataset

2.1 Regional subdivision of the Arctic Ocean: the Central Arctic Ocean and Marginal Seas

The CASPROD database integrates mineralogical and geochemical data covering the entire Arctic Ocean. To facilitate a systematic description and spatial analysis of these datasets, the Arctic Ocean is subdivided into two primary physiographic provinces,

https://doi.org/10.5194/essd-2026-253
Preprint. Discussion started: 20 April 2026

the Central Arctic Ocean and the Arctic Marginal Seas, following the classification scheme proposed by Jakobsson (2002) and Martens et al. (2021). Bathymetric constraints from the General Bathymetric Chart of the Oceans (GEBCO) were employed to delineate the shelf boundaries of these seas (Jakobsson, 2002). Within this framework, the Central Arctic Ocean encompasses the deep abyssal basins, specifically the Canada, Makarov, Amundsen, and Nansen Basins. The Arctic Marginal Seas are characterized by extensive continental shelves surrounding these basins, including the Beaufort, Chukchi, East Siberian, Laptev, Kara, and Barents Seas, as well as the shelf regions adjacent to the Canadian Arctic Archipelago (Figure 1, Table 1).

2.2 Lithological characteristics of the circum-Arctic continents

The mineralogical and geochemical composition of Arctic marine sediments is primarily controlled by the lithology of the surrounding continental source regions. As the principal sediment sources, these geologically diverse provinces bordering the Arctic Ocean impart distinct and diagnostic signatures to the adjacent marine environments (Stein, 2008; Harrison et al., 2008; Pease and Coakley, 2018).

The North American sector, encompassing the Canadian Arctic Archipelago and northern Alaska, is characterized by Precambrian rocks of the Canadian Shield, Paleozoic sedimentary successions of the Arctic Platform, and Mesozoic-Cenozoic orogenic belts associated with the North American Cordillera (Harrison et al., 2008). Geochemically, these ancient continental terrains are characterized by strongly negative εNd values and highly radiogenic $^{87}Sr/^{86}Sr$ ratios. They serve as the primary source of Precambrian zircons and contribute substantial amounts of detrital carbonate minerals (e.g., dolomite and calcite) to the Arctic Ocean.

In contrast, the Eurasian sector exhibits a markedly different geological framework. The large drainage basins of major Siberian rivers, including the Ob, Yenisei, Lena and Kolyma rivers, erode the Mesozoic-Cenozoic sedimentary sequences of the Verkhoyansk-Chukotka region and extensive volcanic provinces, such as the Okhotsk-Chukotka Volcanic Belt (OCVB), the Kolyma-Omolon Belt and the Siberian Traps (Toro et al., 2016). As a result, sediments originating from these regions commonly yield more radiogenic εNd values, less radiogenic $^{87}Sr/^{86}Sr$ ratios, and abundant Mesozoic–Cenozoic zircon populations. Mineralogically, the Eurasian sector represents a major source of characteristic clay minerals, including illite derived from sedimentary rocks and smectite produced by the weathering of basalts, as well as

https://doi.org/10.5194/essd-2026-253
Preprint. Discussion started: 20 April 2026

distinctive detrital minerals (Stein, 2008). Furthermore, the Siberian and Baltic Cratons contribute materials derived from high-grade metamorphic rocks to the Laptev, Kara and Barents Seas. This pronounced lithological heterogeneity establishes unique sediment-source fingerprints for each marginal seas.

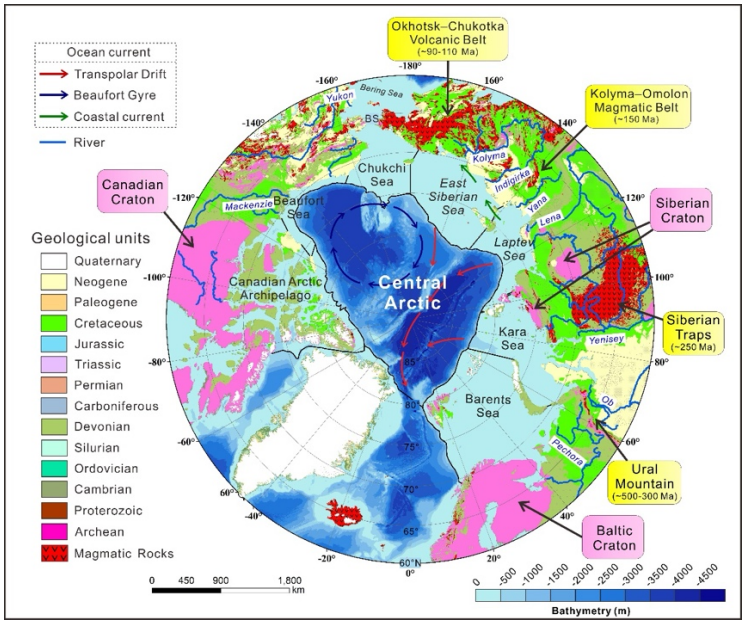

Figure 1. Overview map of the Arctic Ocean illustrating regional subdivisions and circum-Arctic lithological frameworks. The study area is divided into the central Arctic Ocean and the Arctic marginal seas. The geological background is adapted from Harrison et al. (2011). Major magmatic and volcanic belts and cratons (Akinin et al., 2020) are indicated by arrows and annotated with colored boxes. BS denotes the Bering Strait.

2.3 Dataset description

Surface sediment samples included in the CASPROD database were primarily collected from the uppermost layers (typically 0-2 cm to 0-5 cm). For sediment cores, the core-top intervals were used to represent the modern sedimentary conditions. All datasets are provided in standardized data table (Table 2) with a uniform metadata structure containing the following categories and fields. Station metadata: station identifier ("STATION"), geographical coordinates ("LAT" and "LON"), geographic

https://doi.org/10.5194/essd-2026-253
Preprint. Discussion started: 20 April 2026

region ("REGION"), sample position within the core or sediment column ("SAMPLE_PS"). Bathymetric information: water depth derived from shipboard measurement ("WATER_DEPTH") and from the GEBCO bathymetry ("GEBCO_DEPTH"). Water depth values were preferentially obtained from the original publications or cruise reports. For stations where shipboard depth information was unavailable, water depth was estimated using the GEBCO bathymetric grid. Provenance metadata: sample pretreatment methods ("PRETREATMENT"), analytical instrumentation ("INSTRUMENT"), and data source ("REFERENCE").

Table 1. CASPROD data from the central Arctic Ocean and marginal seas

Region*	Area* $10^3 km^2$	Sr-Nd isotope	Detrital zircon U-Pb Age	Clay minerals	Detrital minerals (XRD)	Detrital minerals (Counting)
1. Barents Sea	1626	12	1 (185)**	458	78	505
2. Kara Sea	942	15	5 (1263)	190	31	278
3. Laptev Sea	505	47	4 (846)	138	23	135
4. East Siberian Sea	1000	32	9 (1979)	113	27	533
5. Chukchi Sea	639	21	2 (398)	267	70	432
6. Beaufort Sea	183	4	1 (291)***	294	25	2
7. Canadian Arctic Archipelago	1171	9	0	6	55	0
8. Central Arctic Ocean	4500	35	0	181	168	103
Total（1-8）	10 566	175	21 (4671)	1647	477	1988

* Regional classification and corresponding area follow Martens et al. (2021). ** Numbers outside the parentheses indicate the number of samples, while numbers inside the parentheses denote the number of detrital zircon grains. *** The detrital zircon U-Pb age data for the Beaufort Sea were not obtained from the original source (Rino et al., 2004) and thus were not included in the total age statistics.

https://doi.org/10.5194/essd-2026-253
Preprint. Discussion started: 20 April 2026

199 Table 2. Description of parameters and corresponding column headers in the
200 CASPROD dataset

Parameters	Description	Column name
Sampling and Georeference information		
CASPROD entry ID	Serial number	ID
Station identifier	Expedition station ID	STATION
Latitude	Decimal latitude (WGS1984)	LAT
Longitude	Decimal longitude (WGS1984)	LON
Region	Central Arctic Ocean or marginal seas	REGION
Water depth (m.b.s.l.)	Water depth from shipboard measurement	WATER_DEPTH
Water depth based on GEBCO (m.b.s.l.)	Water depth according to GEBCO	GEBCO_DEPTH
Sample position (cm)	Sample depth below sediment-water interface	SAMPLE_PS
Sample Pretreatment	Chemical pre-treatment method	PRETREATMENT
Analytical Instrument	Instrument used for analysis	INSTRUMENT
Reference	Original publication of the data	REFERENCE
Sr-Nd isotopic data		
$^{87}Sr/^{86}Sr$	Measured $^{87}Sr/^{86}Sr$ ratio	SR
$^{144}Nd/^{143}Nd$	Measured $^{144}Nd/^{143}Nd$ ratio	ND
2σ	Two standard deviations	2S
εNd	$\varepsilon Nd = (^{143}Nd/^{144}Nd - 0.512638) / 0.512638 \times 10000$ (Jacobsen and Wasserburg, 1980)	εND
Zircon U-Pb data		
Zircon number	Number of zircon grains dated per sample	Z_NUM
90-110 Ma proportion	Proportion of 90-110 Ma zircon grains	90_110MA
140-160 Ma proportion	Proportion of 140-160 Ma zircon grains	140_160MA
220-360 Ma proportion	Proportion of 220-360 Ma zircon grains	220_360MA
420-560 Ma proportion	Proportion of 420-560 Ma zircon grains	420_560MA
1000-1500 Ma proportion	Proportion of 1000-1500 Ma zircon grains	1000_1500MA
1750-2000 Ma proportion	Proportion of 1750-2000 Ma zircon grains	1750_2000MA
Clay mineral data		
Smectite (%)	Smectite content	SME
Illite (%)	Illite content	ILL
Kaolinite (%)	Kaolinite content	KAO

https://doi.org/10.5194/essd-2026-253
Preprint. Discussion started: 20 April 2026

Chlorite (%)	Chlorite content	CHL
Sample grain size	Particle size range used for testing	GS
Diffractometer	Diffractometer for testing	DFM
Slit	Slit used during testing	SLIT
Calculation software	Software for calculating mineral content	SOFTWARE
Comments	Necessary supplements	COMMENTS
Detrital mineral data		
Quartz (%)	Quartz content	QZ
Plagioclase feldspar (%)	Plagioclase feldspar content	PI
Potassium feldspar (%)	Potassium feldspar content	KFS
Calcite (%)	Calcite content	CAL
Dolomite (%)	Dolomite content	DOL
Siderite (%)	Siderite content	SD
Muscovite (%)	Muscovite content	MU
Biotite (%)	Biotite content	BI
Glauconite (%)	Glauconite content	Glt
Pyroxene (%)	Pyroxene content	PX
Amphibole (%)	Amphibole content	AM
Garnet (%)	Garnet content	GRT
Staurolite (%)	Staurolite content	ST
Andalusite (%)	Andalusite content	AND
Kyanite (%)	Kyanite content	KY
Sillimanite (%)	Sillimanite content	SIL
Epidote (%)	Epidote content	EP
Chloritoid (%)	Chloritoid content	CLD
Prehnite (%)	Prehnite content	PRH
Zeolite (%)	Zeolite content	ZEO
Serpentine (%)	Serpentine content	SRP
Actinolite (%)	Actinolite content	ACT
Zircon (%)	Zircon content	ZRN
Tourmaline (%)	Tourmaline content	TUR
Rutile (%)	Rutile content	RT
Titanite (%)	Titanite content	TTN
Apatite (%)	Apatite content	AP
Anatase (%)	Anatase content	ANT
Magnetite (%)	Magnetite content	MAG
Hematite (%)	Hematite content	HEM
Limonite (%)	Limonite content	LIM
Ilmenite (%)	Ilmenite content	ILM

https://doi.org/10.5194/essd-2026-253
Preprint. Discussion started: 20 April 2026

Pyrite (%)	Pyrite content	PY
Barite (%)	Barite content	BRT
Spinel (%)	Spinel content	SPL

2.4 Dataset parameters

The CASPROD database integrates four primary provenance proxy categories, providing key multi-proxy data to constrain sediment sources and transport pathways within the Arctic Ocean: Sr–Nd isotopes, detrital zircon U–Pb ages, clay mineral assemblages, and detrital mineral compositions (Table 2). The clay mineralogy dataset reports the relative abundances of four major groups: kaolinite, illite, smectite, and chlorite. The detrital mineral dataset comprises a diverse suite of mineral types, generally categorized into heavy- and light-mineral fractions (Table 2). All compiled datasets are publicly accessible through the repository described in the Data Availability section.

2.5 Data sources and quality assurance

The CASPROD dataset synthesizes data from 117 previously published studies and publicly available databases, all of which are fully and appropriately cited. To ensure complete traceability, each data record is explicitly linked to its original source reference within the primary data tables. A comprehensive bibliography of all source publications is provided in the Supplement. Furthermore, to enable rigorous user-assessed quality, the database documents detailed metadata for each record. For detrital zircon and detrital mineral data obtained through microscopic identification, the corresponding pre-treatment methods and instruments are provided. For clay mineral and detrital data derived from XRD analysis, the dataset includes pre-treatment procedures, XRD instruments (including the type of X-ray tube, e.g., Cu or Co), whether the slit system is automatic or fixed, and the software used for data calculation.

2.6 Data interpolation

To facilitate spatial analysis and visualization, the CASPROD database provides interpolated raster products (GeoTIFF format) for Sr-Nd isotopes, clay mineral assemblages, and detrital mineral distributions. All spatial data are projected using the

https://doi.org/10.5194/essd-2026-253
Preprint. Discussion started: 20 April 2026

WGS 1984 Arctic Polar Orthographic projection to minimized distortion at high latitudes. Interpolation was performed using Ocean Data View software (ODV; Schlitzer, 2022), specifically employing the Data-Interpolating Variational Analysis (DIVA) method (Brasseur et al., 1996; Troupin et al., 2012). DIVA is a variational interpolation technique that estimates continuous fields by optimizing a cost function to balances data fidelity, field smoothness, and consistency with physical boundaries constraints such as complex coastlines. In contrast to traditional kriging methods, DIVA explicitly accounts for anisotropic spatial correlations and incorporates boundary conditions, making it exceptionally suitable for oceanographic datasets characterized by complex basin geometries and irregular data coverage. As implemented in ODV, DIVA allows user-defined correlation lengths in both longitudinal and latitudinal directions, generates gridded estimation error fields, and supports isopycnic gridding when density-based coordinates are applied. Consequently, this approach improves the representation of spatial gradients in regions with heterogeneous data coverage, particularly between the Arctic shelf seas and central deep basins.

3. Results and discussion

3.1 Dataset inventory and spatial distribution

This section presents an overview of the CASPROD database inventory and examines the spatial distribution of the four primary provenance proxy groups across the Arctic Ocean. By systematically mapping the data coverage across the Arctic Ocean, we highlight regional variations in data density and identify areas where information remains limited. The geographical patterns of key geochemical and mineralogical parameters are illustrated using a series of maps and diagrams.

3.1.1 Sr-Nd Isotopes

The Sr-Nd isotopic dataset comprises 175 data points from detrital component of surface sediments, with εNd values ranging from -19.5 to -4.0 and $^{87}Sr/^{86}Sr$ ratios from 0.710 to 0.745. A composite map that overlays all sample locations with the interpolated spatial distributions of $^{87}Sr/^{86}Sr$ ratio and εNd values, revealing a pronounced contrast between the two major Arctic sectors (Figure 2). The North American sector exhibits higher $^{87}Sr/^{86}Sr$ ratios and lower εNd values relative to the Eurasian sector. Specifically,

https://doi.org/10.5194/essd-2026-253
Preprint. Discussion started: 20 April 2026

Open Access Earth System Science Data Discussions

the North American margin features evolved crustal signals, with mean values observed in the Canadian Arctic Archipelago (εNd = -14.7, $^{87}Sr/^{86}Sr$ = 0.728), and Beaufort Sea (εNd= -14.4, $^{87}Sr/^{86}Sr$ = 0.731). In contrast, sediments from the Eurasian marginal seas exhibit systematically higher εNd values and lower $^{87}Sr/^{86}Sr$ ratios. Representative mean values include the Barents Sea (εNd = -10.7, $^{87}Sr/^{86}Sr$ = 0.722), Kara Sea (εNd = -7.9, $^{87}Sr/^{86}Sr$ = 0.717), Laptev Sea (εNd = -12.0, $^{87}Sr/^{86}Sr$ = 0.716), East Siberian Sea (εNd = -9.5, $^{87}Sr/^{86}Sr$ = 0.714), and Chukchi Sea (εNd = -8.0, $^{87}Sr/^{86}Sr$ = 0.712).

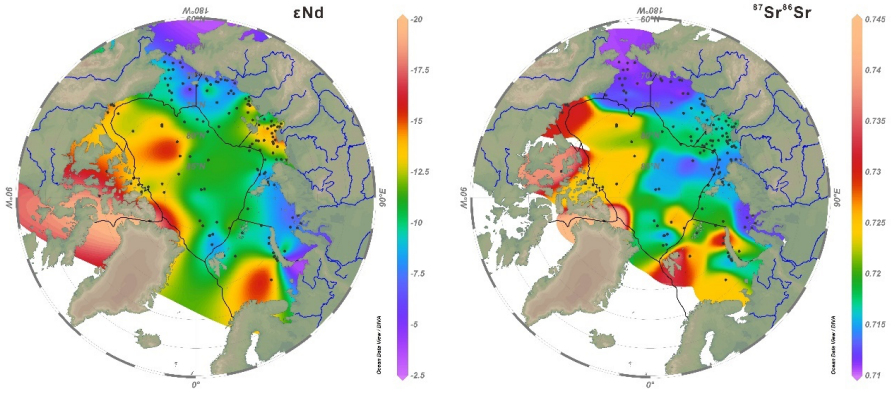

Figure 2. Spatial distribution of εNd and $^{87}Sr/^{86}Sr$ in surface sediments of the Arctic Ocean

3.1.2 Zircon U-Pb Ages

The detrital zircon U-Pb ages dataset comprises 22 surface sediment samples, yielding 4671 ages. Age distributions for each marginal seas are visualized using frequency histograms and kernel density estimation (KDE) plots (Figure 3). While original zircon age data for the Beaufort Sea are unavailable, the zircon age distribution was derived by digitizing the figure from Rino et al. (2004). These distribution patterns reveal distinct regional provenance signatures across the circum-Arctic marginal seas. A common Paleoproterozoic age peak at ~1750–2000 Ma is evident throughout the Arctic basin, whereas the North American sector is uniquely characterized by a Mesoproterozoic population (1000–1500 Ma) that is absent in Eurasian margin sediments. In contrast, sediments from the Eurasian marginal seas display distinctive younger zircon age populations. The Barents and Kara Seas are characterized by

https://doi.org/10.5194/essd-2026-253
Preprint. Discussion started: 20 April 2026

prominent peaks at 220–360 Ma and 420–560 Ma, whereas the Laptev Sea shows dominant populations at 140–160 Ma and 220–360 Ma. Even younger detrital zircon signatures are evident in the East Siberian and Chukchi Seas, where age spectra are dominated by a pronounced peak at 90–110 Ma.

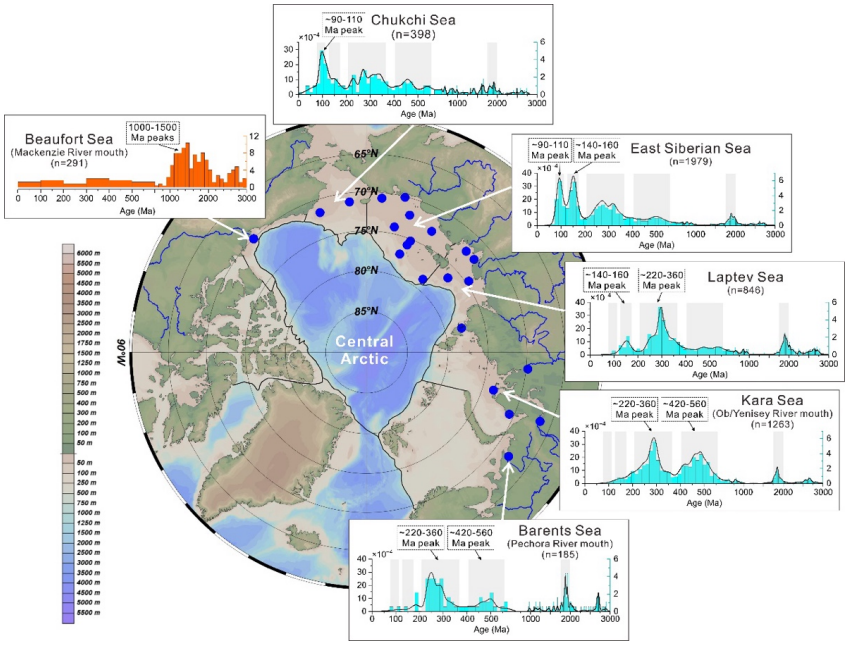

Figure 3. Station map and detrital zircon U-Pb age distribution in surface sediments of the Arctic Ocean

3.1.3 Clay Mineral Assemblages

The clay mineralogy dataset (n=1647) records the relative abundances (%) of four principal mineral groups: illite, smectite, kaolinite, and chlorite. Spatially interpolated maps for each mineral (Figure 4) reveal distinct basin-scale fractionation patterns. Smectite concentrations are notably higher in the Kara Sea (mean 38.9%), with secondary peaks in the Canadian Arctic Archipelago (17.2%), and the Laptev Sea (17.7%). Kaolinite is elevated primarily in the Barents Sea (14.0%) and the Beaufort Sea (10.6%), while illite dominates the eastern Arctic, particularly in the East Siberian (66.3%), Beaufort (60.6%) Seas and Chukchi (53.8%). Unlike the other minerals, chlorite displays a relatively uniform distribution throughout the Arctic marginal seas, with average values ranging narrowly from 17.3% to 23.3%. These mean values for the

https://doi.org/10.5194/essd-2026-253
Preprint. Discussion started: 20 April 2026

298 circum-Arctic marginal seas are quite similar to those listed in Stein (2008).

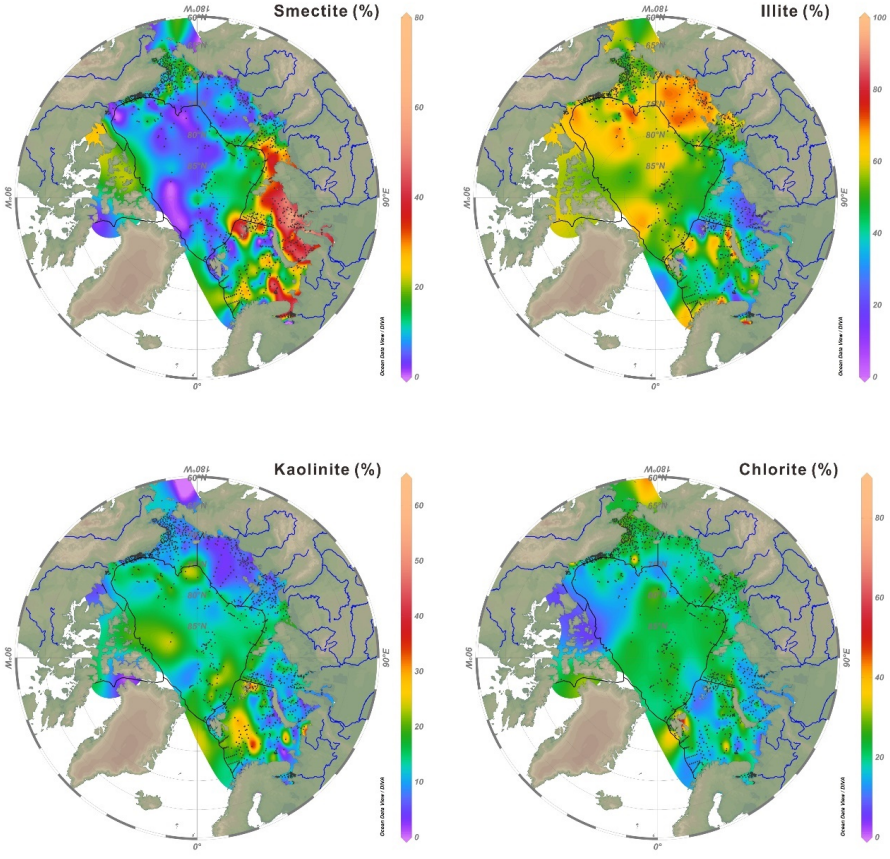

299

300 Figure 4. Spatial distribution of major clay minerals (Smectite, Illite, Kaolinite, and
301 Chlorite) in surface sediments of the Arctic Ocean.

302 *3.1.4 Detrital Mineral Assemblages*

303 The detrital mineral dataset contains 2465 analyses that characterize both light
304 (e.g., quartz, feldspar, dolomite) and heavy mineral fractions (e.g., amphibole, pyroxene,
305 garnet, staurolite). These data were obtained using from two complementary analytical
306 approaches: X-ray diffraction (XRD, n=477) and optical counting (n=1988). Figure 5
307 presents distribution maps of key provenance-sensitive minerals, illustrating significant
308 regional heterogeneity across the Arctic margins. Among the light minerals fraction,
309 quartz is most abundant in the Beaufort (35.9%), Kara (34.2%), and Laptev (33.8%)
310 Seas. Plagioclase enrichment is characteristic of the Laptev (25.8%), Kara (22.9%), and

https://doi.org/10.5194/essd-2026-253
Preprint. Discussion started: 20 April 2026

East Siberian (19.5%) Seas, whereas potassium feldspar (K-feldspar) concentrations are elevated in the Canadian Arctic Archipelago (10.0%), the Laptev Sea (8.9%), and the Kara Sea (6.7%). Notably, carbonate signals, specifically dolomite, are distinctly enriched in the North American sector, the Canadian Arctic Archipelago (11.0%) and the Beaufort Sea (5.5%).

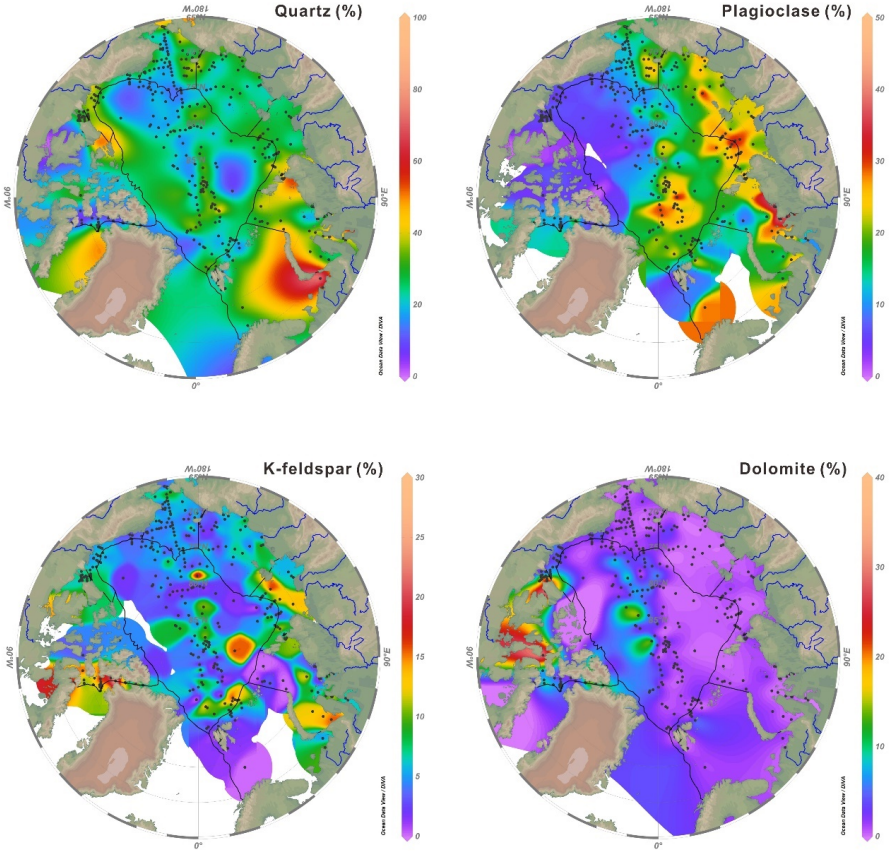

Figure 5. Spatial distribution of key light minerals (Quartz, Plagioclase, K-feldspar, and Dolomite) in surface sediments of the Arctic Ocean.

Within the heavy mineral fraction, pyroxene concentrations peak in the eastern Arctic, notably the Kara (20.5%) and Laptev Seas (20.2%), as well as in areas adjacent to Franz Josef Island near the Kara-Barents sector. Amphibole dominates the heavy mineral fraction in the Laptev Sea (27.4%), followed by the East Siberian Sea (17.7%),

https://doi.org/10.5194/essd-2026-253
Preprint. Discussion started: 20 April 2026

and the Chukchi Sea (14.8%), and is also rich in southern Barents Sea. Metamorphic indicators, such as garnet, are elevated in the Barents (8.9%), Laptev (7.1%), and Kara (5.6%) Seas, while epidote shows relative enrichment in the Chukchi (19.7%) and Barents Seas (11.9%).

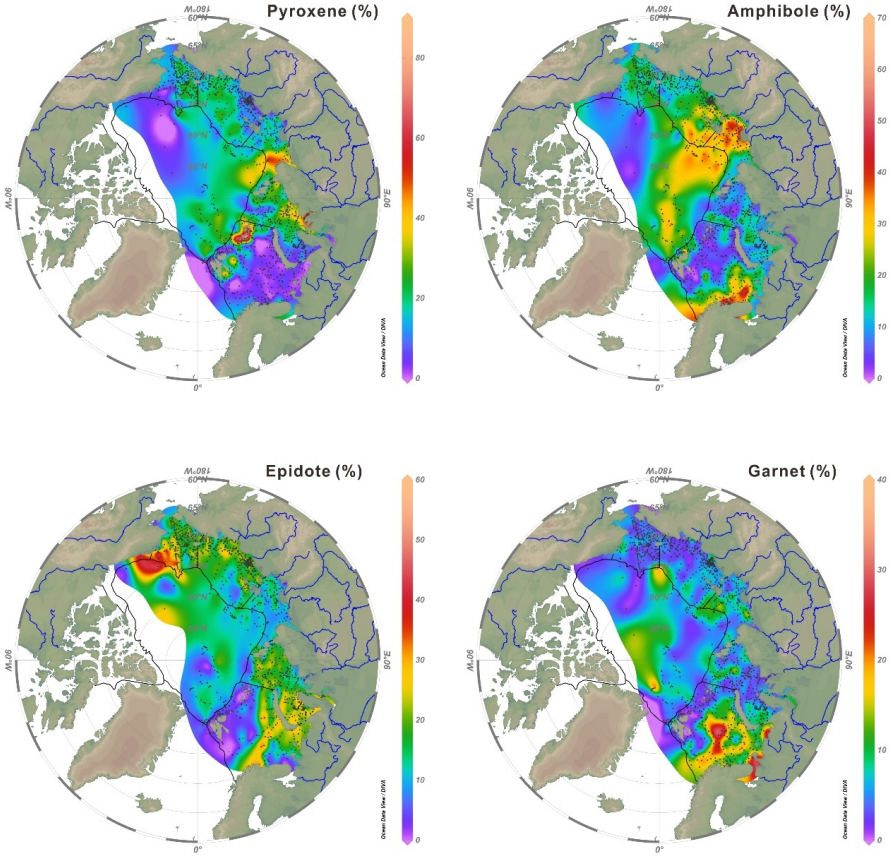

Figure 6. Spatial distribution of key heavy minerals (Pyroxene, Amphibole, Epidote, and Garnet) in surface sediments of the Arctic Ocean.

3.2 *Circum-Arctic provenance implications*

The provenance proxies in the CASPROD database facilitate constraining sediment sources by correlating shelf deposits with the geological characteristics of their respective hinterlands. These distinct geochemical and mineralogical “fingerprints”

https://doi.org/10.5194/essd-2026-253
Preprint. Discussion started: 20 April 2026

336 also serve as critical tracers for basin-scale sediment transport processes. The Sr-Nd
337 isotopic compositions reflect the crustal residence age of source rocks (White, 2013).
338 High $^{87}Sr/^{86}Sr$ ratios and low εNd values in the Canadian Arctic Archipelago, Beaufort,
339 Barents, and Laptev Seas define a characteristic "cratonic" signature, indicative of
340 sediment contributions from ancient Archean basement rocks, including North America,
341 Baltica, and Siberia (Bazhenova et al., 2017). Conversely, the Eurasian sector is
342 characterized by “younger” isotopic signatures. Low $^{87}Sr/^{86}Sr$ and relatively high εNd
343 values in the Kara Sea are consistent with sediment inputs derived from the Permian-
344 Triassic Siberian Large Igneous Province (SLIP; Tütken et al., 2002), while similar
345 isotopic signatures in the East Siberian and Chukchi Seas originate from the Jurassic-
346 Cretaceous OCVB (Li et al., 2023).

347 Zircon U-Pb age spectra provide further constrain on sediment provenance by
348 identifying the formation ages of felsic igneous rocks in the source regions (Moecher
349 and Samson, 2006). The North American sector, particularly sediments influenced by
350 the Mackenzie River system, is uniquely characterized by a prominent 1000–1500 Ma
351 age population, diagnostic of the Grenville Orogeny (Rino et al., 2004). In contrast,
352 zircon age distributions from the Eurasian sector are dominated by Phanerozoic
353 populations, including: (1) 420–560 Ma peaks in the Barents and Kara Seas, likely
354 correlating with the erosion of the Ural Mountains or the Central Asian Orogenic Belt
355 (Puchkov and Ivanov, 2020; Parfenov et al., 2009; (2) 220–360 Ma age populations in
356 the Barents, Kara, and Laptev Seas, consistent with contributions from the SLIP or the
357 Central Asian Orogenic Belt (Campbell et al., 1992); and (3) 90–160 Ma age
358 populations in the East Siberian, Chukchi, and Laptev Seas, which clearly trace
359 magmatic activity associated with the OCVB (Akinin et al., 2020).

360 Clay and detrital mineral assemblages provide complementary insights into
361 lithology. Smectite, commonly produced during chemical weathering of mafic
362 substrates (Wilson, 2004), is enriched in the Kara and Laptev Seas, reflecting erosion
363 of basalts from the SLIP basalts (e.g., Rossak et al., 1999; Wahsner et al., 1999; Stein
364 et al., 2004). Similarly, elevated smectite abundances in the Canadian Arctic
365 Archipelago similarly indicate the local erosion of exposed mafic gabbros (Kingsbury

https://doi.org/10.5194/essd-2026-253
Preprint. Discussion started: 20 April 2026

et al., 2018). Kaolinite, by contrast, reflects reworking of ancient weathering crusts formed under warm and humid climatic conditions. Important sources include Triassic and Jurassic sedimentary rocks on Franz Josef Land (Elverhøi et al., 1989; Vogt and Knies, 2009) and the deeply weathered North American Craton supplying sediments to the Canadian Arctic Archipelago (Stevenard et al., 2022). Hight illite contents in the East Siberian, Chukchi, and Beaufort Seas are indicative of dominant physical weathering of mixed sedimentary, metamorphic, and felsic igneous lithologies (e.g., Viscosi-Shirley et al., 2003; Stein, 2008).

Light mineral assemblages further refine provenance interpretations. Plagioclase, indicative of relatively unweathered igneous sources (Dickinson, 1985), is particularly enriched in the Kara, Laptev, and East Siberian Seas, reflecting inputs from the SLIP and OCVB. Potassium feldspar indicates granitic or gneissic sources, linking sediments in the Laptev Sea and western Kara Seas to erosion of the Siberian Craton and Uralian basement, respectively (Vogt, 1997). Quartz dominates in regions with limited igneous influence, such as areas affected by the Pechora River and Mackenzie River system and the Taimyr-Severnaya Zemlya fold belt. Dolomite enrichment in the Canadian Arctic Archipelago provides a clear fingerprint of local Cambrian-Devonian carbonate bedrocks erosion (Clark et al., 1980; Vogt, 1997; Phillips and Grantz, 2001; Stein et al., 2010; Bazhenova et al., 2017). Within the heavy mineral fraction, pyroxene serves as a diagnostic mafic tracer (Garzanti and Andò, 2007), linking sediments near Franz Josef Land to local mafic igneous outcrops and sediments in the Kara and Laptev Seas to erosion of the Siberian Traps (Behrends, 1999; Wang et al., 2022). High-grade metamorphic indicator minerals, such as garnet and amphibole (Behrends, 1999; Garzanti and Andò, 2007), are abundant in the Barents, Kara, and Laptev Seas, reflecting erosion of crystalline basement from the Baltic and Siberian Cratons, especially the Taimyr region.

Stein (2008) documented the spatial distribution patterns of four clay minerals (illite, smectite, chlorite, and kaolinite) and four detrital minerals (amphibole, clinopyroxene, epidote, and garnet) across the Arctic Ocean (for database and download see Stein, 2026a, 2026b). Furthermore, lower-resolution distribution maps of the

https://doi.org/10.5194/essd-2026-253
Preprint. Discussion started: 20 April 2026

detrital minerals quartz, plagioclase, kalifeldspar and dolomite of surface sediments from the central Arctic Ocean and the Laptev and Kara seas are also presented in Stein (2008), based on data from Vogt (1997). Compared with the database compiled by Stein (2008), the overall spatial distribution patterns as well as mean concentrations of both clay and detrital minerals in our new dataset remain largely consistent, confirming the robustness of the earlier synthesis of mineralogy. However, the present compilation incorporates recently published data from the Canada Basin (e.g., Deschamps et al., 2018), the Canadian Arctic Archipelago (e.g., Myers et al., 2022), the Chukchi Sea (e.g., Li et al., 2021), the East Siberian Sea (e.g., Wang et al., 2024), and the Barents Sea (e.g., Vogt and Knies, 2009), thereby improving spatial coverage across key Arctic marginal seas. The inclusion of these new datasets enables a higher-resolution and more refined characterization of mineral distribution patterns in regions that were less well constrained in Stein (2008), particularly over the East Siberian Sea shelf and within the Canada Basin. In addition, we expand the analysis to include a broader suite of provenance-sensitive detrital minerals, such as quartz, plagioclase, K-feldspar, dolomite, pyroxene, and staurolite, further strengthening source-to-sink interpretations.

These provenance signals extend beyond the continental shelves into the central Arctic Ocean, delineating modern sediment transport pathways. The Canada Basin exhibits geochemical and mineralogical signatures closely resembling those of the North American margins (the CAA and the Beaufort Sea), reflecting sediment transport mediated by the clockwise Beaufort Gyre. Conversely, the Eurasian Basin mirrors the provenance characteristics of the Eurasian shelves, reflecting sediment entrainment and export by the Transpolar Drift (Timmermans and Marshall, 2020). This pronounced basin-scale dichotomy establishes a robust baseline for using surface-sediment provenance proxies of surface sediment to reconstruct Quaternary ice dynamics and the transport pathways of icebergs calved from surrounding ice-sheets (e.g., Darby et al., 2012; Xiao et al., 2021; Feng et al., 2025; Stein et al., 2025).

4. Data availability

The CASPROD dataset is publicly available at Figshare (https://doi.org/10.6084/m9.figshare.31926927; Yao et al., 2026) and is provided under

https://doi.org/10.5194/essd-2026-253
Preprint. Discussion started: 20 April 2026

an open-access license. All relevant contact information and metadata documentation are provided on the website. The scientific community is encouraged to contribute new and updated datasets to CASPROD, enabling continuous expansion and updates of this resource.

5. Conclusions and outlook

The CASPROD database is one of the most comprehensive compilations of sensitive provenance-related data for Arctic surface sediments currently available. By integrating mineralogical parameters with key geochemical tracers, such as Sr-Nd isotopes and detrital zircon U-Pb ages, CASPROD establishes a valuable framework for characterizing sediment sources across the circum-Arctic margins. While individual provenance proxies reflect specific aspects of source lithology and weathering regimes, these signals are inherently modified by sediment mixing, transport processes (riverine input, sea-ice rafting and ocean circulation), and hydrodynamic sorting within the Arctic Ocean. As a result, interpretations based on a single proxy can be ambiguous, particularly in regions where source signatures overlap. The multi-proxy strategy implemented in CASPROD is therefore essential. Integrating complementary tracers improves the discrimination of potential sources and enables quantitative unmixing, provided end-member compositions are well-constrained. Ultimately, this integrated framework not only elucidates modern sediment source-to-sink process but also provides a critical baseline for reconstructing Quaternary environmental changes, including ice-sheet dynamics, sea-ice variability, and ocean circulation. As such, CASPROD constitutes a valuable and enduring resource for advancing research in Arctic marine geology, paleoclimatology, and Earth system science.

Supplement. The supplementary materials related to this article is available online.

Author Contributions. ZY conceived and designed the study. ZY and HF were responsible for the construction of the database. RS, YL, XS, YV, SN, LD, FS, KW, ZC, SQ, QL, SZ, XP, HG, YL contributed to data collection, database construction, and verification. ZY drafted the manuscript. All authors contributed to the writing and editing of the manuscript.

https://doi.org/10.5194/essd-2026-253
Preprint. Discussion started: 20 April 2026

Competing interests. The authors declare that they have no conflict of interest.

Acknowledgements. We thank the crew members and scientific participants of the Chinese-Russian joint expedition cruises and the Chinese Arctic Research Expeditions for their efforts in sampling collection. We are also grateful to the scientists who contributed data to the CASPROD database. We are particularly indebted to Christoph Vogt for his guidance in compiling the clay mineral dataset. This work was supported by the National Natural Science Foundation of China (42525606), the National Key Research and Development Program of China (2023YFF0804600), and the Russian state budget (124022100084-8 of the POI FEB RAS).

References

Akinin, V. V., Miller, E. L., Toro, J., Prokopiev, A. V., Gottlieb, E. S., Pearcey, S., Polzunenkov, G. O., and Trunilina, V. A.: Episodicity and the dance of late Mesozoic magmatism and deformation along the northern circum-Pacific margin: north-eastern Russia to the Cordillera, Earth Sci. Rev., 208, 103272, https://doi.org/10.1016/j.earscirev.2020.103272, 2020.

Andrews, J. T.: Baffin Bay/Nares Strait surface (seafloor) sediment mineralogy, Further investigations and methods to elucidate spatial variations in provenance, Can. J. Earth Sci., 56, 814-828, https://doi.org/10.1139/cjes-2018-0207, 2019.

Bazhenova, E. A.: Reconstruction of late Quaternary sedimentary environments at the southern Mendeleev Ridge (Arctic Ocean), Ph.D. thesis, Fakultät für Geowissenschaften, University of Bremen, Bremen, Germany, 83 pp., https://hdl.handle.net/10013/epic.dec92c3a-3ec6-4ead-87e1-bd77301c604c, 2012.

Bazhenova, E., Fagel, N., and Stein, R.: North American origin of "pink–white" layers at the Mendeleev Ridge (Arctic Ocean): New insights from lead and neodymium isotope composition of detrital sediment component, Mar. Geol., 386, 44-55, https://doi.org/10.1016/j.margeo.2017.01.010, 2017.

Behrends, M.: Reconstruction of sea-ice drift and terrigenous sediment supply in the Late Quaternary: Heavy-mineral associations in sediments of the Laptev-Sea continental margin and the central Arctic Ocean, Reps. Pol. Res., 310, 167 pp.,

https://doi.org/10.5194/essd-2026-253
Preprint. Discussion started: 20 April 2026

https://epic.awi.de/id/eprint/26490/, 1999.

Brasseur, P., Beckers, J.-M., Brankart, J.-M., and Schoenauen, R.: Seasonal temperature and salinity fields in the Mediterranean Sea: Climatological analyses of an historical data set, Deep-Sea Res. Pt. I, 43, 159–192, https://doi.org/10.1016/0967-0637(96)00012-X, 1996.

Campbell, I. H., Czamanske, G. K., Fedorenko, V. A., Hill, R. I., and Stepanov, V.: Synchronism of the Siberian Traps and the Permian-Triassic Boundary, Sci., 258, 1760-1763, https://doi.org/10.1126/science.258.5089.1760, 1992.

Clark, D. L., Whitman, R. R., Morgan, K. A., and Mackey, S. D.: Stratigraphy and glacial marine sediments of the Amerasian Basin, central Arctic Ocean, Geol. Soc. Am. Spec. Pap. 181, 57 pp., https://doi.org/10.1130/SPE181-p1, 1980.

Cohen, J., Screen, J. A., Furtado, J. C., Barlow, M., Whittleston, D., Coumou, D., Francis, J., Dethloff, K., Entekhabi, D., Overland, J., and Jones, J.: Recent Arctic amplification and extreme mid-latitude weather. Nat. Geosci., 7, 627-637, https://doi.org/10.1038/ngeo2234, 2014.

Darby, D. A., Ortiz, J. D., Grosch, C. E., and Lund, S. P.: 1,500-year cycle in the Arctic Oscillation identified in Holocene Arctic sea-ice drift, Nat. Geosci., 5, 897-900, https://doi.org/10.1038/ngeo1629, 2012.

Darby, D. A.: Sources of sediment found in sea ice from the western Arctic Ocean: New insights into processes of entrainment and drift patterns, J. Geophys. Res. Oceans, 108, 3257, https://doi.org/10.1029/2002JC001350, 2003.

Deschamps, C., Montero-Serrano, J., and St-Onge, G.: Sediment Provenance Changes in the Western Arctic Ocean in Response to Ice Rafting, Sea Level, and Oceanic Circulation Variations Since the Last Deglaciation, Geochem. Geophy. Geosy., 19, 2147-2165, https://doi.org/10.1029/2017GC007411, 2018.

Dickinson, W. R.: Interpreting provenance relations from detrital modes of sandstones, in: Provenance of Arenites, edited by: Zuffa G. G., Springer Netherlands, Dordrecht, 333-361, https://doi.org/10.1007/978-94-017-2809-6_15, 1985.

Dong L., Shi X., Liu Y., Fang X., Chen Z., Wang C., Zou J., Huang Y.: Minerals in surface sediments in the western Arctic Ocean and their sources (in Chinese), Chin.

https://doi.org/10.5194/essd-2026-253
Preprint. Discussion started: 20 April 2026

J. Polar Res., 26, 58-70, https://doi.org/10.13679/j.jdyj.2014.1.058, 2014.

Eicken, H., Gradinger, R., Gaylord, A., Mahoney, A., Rigor, I., and Melling, H.: Sediment transport by sea ice in the Chukchi and Beaufort Seas: Increasing importance due to changing ice conditions?, Deep-Sea Res. Pt. II, 52, 3281-3302, https://doi.org/10.1016/j.dsr2.2005.10.006, 2005.

Elverhøi, A., Pfirman, S. L., Solheim, A., and Larssen, B. B.: Glaciomarine sedimentation in epicontinental seas exemplified by the northern barents sea, Mar. Geol., 85, 225-250, https://doi.org/https://doi.org/10.1016/0025-3227(89)90155-2, 1989.

Fedo, C. M., Sircombe, K. N., and Rainbird, R. H.: Detrital zircon analysis of the sedimentary record, Rev. Mineral. Geochem., 53, 277-303, https://doi.org/10.2113/0530277, 2003.

Feng, H., Yao, Z., Shi, X., Zhang, Z., Lu, H., Zhang, H., Liu, Y., Shan, X., Dong, J., Dong, L., Yang, G., Hu, L., Vasilenko, Y., Astakhov, A., and Bosin, A.: Arctic zircon U-Pb ages reveal multiphase glaciations in East Siberia during the late Quaternary, Nat. Commun., 16, 7511, https://doi.org/10.1038/s41467-025-62499-y, 2025.

Ford, D., and Golonka, J.: Phanerozoic paleogeography, paleoenvironment and lithofacies maps of the circum-Atlantic margins, Mar. Pet. Geol., 20, 249-285, https://doi.org/10.1016/S0264-8172(03)00041-2, 2003.

Gamboa, A., Montero-Serrano, J.-C., St-Onge, G., Rochon, A. and Desiage, P.-A.: Mineralogical, geochemical and magnetic signatures of surface sediments from the Canadian Beaufort Shelf and Amundsen Gulf (Canadian Arctic), Geochemistry, Geophysics, Geosystems, 18, https://doi.org/10.1002/2016GC006477, 2017.

Garzanti, E., and Andò, S.: Heavy mineral concentration in modern sands: Implications for provenance interpretation, in Heavy Minerals in Use, edited by: M. A. Mange and D. T. Wright, Elsevier, 58, 517-545, https://doi.org/10.1016/S0070-4571(07)58020-9, 2007.

Gordeev, V. V.: Fluvial sediment flux to the Arctic Ocean, Geomorphology, 80, 94-104, https://doi.org/10.1016/j.geomorph.2005.09.008, 2006.

https://doi.org/10.5194/essd-2026-253
Preprint. Discussion started: 20 April 2026

546 Harrison, J. C., St-Onge, M. R., Petrov, O., Strelnikov, S., Lopatin, B., Wilson, F., Tella,
547 S., Paul, D., Lynds, T. L., Shokalsky, S., Hults, C., Bergman, S., Jepsen, H. F., and
548 Solli, A.: Geological map of the Arctic, Geol. Surv. Can., Ottawa, Ont., Open File,
549 5816, https://doi.org/10.4095/225705, 2008.
550 Harrison, J., St-Onge, M., Petrov, O., Strelnikov, S., Lopatin, B., Wilson, F., Tella, S.,
551 Paul, D., Lynds, T., Shokalsky, S., Hults, C., Bergman, S., Jepsen, H., and Solli,
552 A.: Geological map of the arctic, Geological Survey of Canada, 2011.
553 Henderson, G. R., Barrett, B. S., Wachowicz, L. J., Mattingly, K. S., Preece, J. R., and
554 Mote, T. L.: Local and remote atmospheric circulation drivers of Arctic change: A
555 review, Front. Earth Sci., 9, 709024, https://doi.org/10.3389/feart.2021.709896,
556 2021.
557 Holmes, R. M., McClelland, J. W., Peterson, B. J., Shiklomanov, I. A., Shiklomanov, A.
558 I., Zhulidov, A. V., Gordeev, V. V., and Bobrovitskaya, N. N.: A circumpolar
559 perspective on fluvial sediment flux to the Arctic Ocean, Global Biogeochem. Cy.,
560 16, 1098, https://doi.org/10.1029/2001GB001849, 2002.
561 IMBIE Team: Mass balance of the Greenland Ice Sheet from 1992 to 2018, Nature, 579,
562 233-239, https://doi.org/10.1038/s41586-019-1855-2, 2020.
563 Jacobsen, S. B. and Wasserburg, G. J.: Sm-Nd isotopic evolution of chondrites, Earth
564 Planet. Sci. Lett., 50, 139-155, https://doi.org/https://doi.org/10.1016/0012-
565 821X(80)90125-9, 1980.
566 Jakobsson, M.: Hypsometry and volume of the Arctic Ocean and its constituent seas,
567 Geochem. Geophy. Geosy., 3, 1-18, https://doi.org/10.1029/2001GC000302, 2002.
568 Jang, K., Bayon, G., Vogt, C., Forwick, M., Ahn, Y., Kim, J.-H. and Nam, S.-I.: Non-
569 linear response of glacier melting to Holocene warming in Svalbard recorded by
570 sedimentary iron (oxyhydr)oxides, Earth and Planet. Sc. Lett., 607, 118054,
571 https://doi.org/10.1016/j.epsl.2023.118054, 2023.
572 Kingsbury, C. G., Kamo, S. L., Ernst, R. E., Söderlund, U., and Cousens, B. L.: U-Pb
573 geochronology of the plumbing system associated with the Late Cretaceous Strand
574 Fiord Formation, Axel Heiberg Island, Canada: Part of the 130-90 Ma High Arctic
575 large igneous province, J. Geodyn., 118, 106-117,

https://doi.org/10.5194/essd-2026-253
Preprint. Discussion started: 20 April 2026

https://doi.org/10.1016/j.jog.2017.11.001, 2018.

Li, Q., Qiao, S., Shi, X., Chen, Y., Astakhov, A., Zhang, H., Hu, L., Yang, G., Bosin, A., Vasilenko, Y., and Dong, L.: Sr, Nd, and Pb isotope provenance of surface sediments on the East Siberian Arctic Shelf and implications for transport pathways, Chem. Geol., 618, 121277, https://doi.org/10.1016/j.chemgeo.2022.121277, 2023.

Li, Q., Qiao, S., Shi, X., Hu, L., Bai, Y., Zhu, A., and Cui, J.: Sediment provenance of the East Siberian Arctic Shelf: Evidence from clay minerals and chemical elements (in Chinese), Acta Oceanol. Sin., 43, 76-89, https://doi.org/10.12284/hyxb2021041, 2021.

Maccali, J., Hillaire-Marcel, C., and Not, C.: Radiogenic isotope (Nd, Pb, Sr) signatures of surface and sea ice-transported sediments from the Arctic Ocean under the present interglacial conditions, Polar Res., 37, 1442982, https://doi.org/10.1080/17518369.2018.1442982, 2018.

Martens, J., Romankevich, E., Semiletov, I., Wild, B., van Dongen, B., Vonk, J., Tesi, T., Shakhova, N., Dudarev, O. V., Kosmach, D., Vetrov, A., Lobkovsky, L., Belyaev, N., Macdonald, R. W., Pieńkowski, A. J., Eglinton, T. I., Haghipour, N., Dahle, S., Carroll, M. L., åström, E. K. L., Grebmeier, J. M., Cooper, L. W., Possnert, G., and Gustafsson, Ö.: Cascade-The circum-Arctic sediment carbon database, Earth Syst. Sci. Data, 13, 2561-2572, https://doi.org/10.5194/essd-13-2561-2021, 2021.

Martinez, N. C., Murray, R. W., Dickens, G. R., and Kölling, M.: Discrimination of sources of terrigenous sediment deposited in the central Arctic Ocean through the Cenozoic, Paleoceanography, 24, PA1210, https://doi.org/10.1029/2007PA001567, 2009.

McCave, I. N., and Andrews, J. T.: Distinguishing current effects in sediments delivered to the ocean by ice. I. Principles, methods and examples, Quat. Sci. Rev., 212, 92-107, https://doi.org/10.1016/j.quascirev.2019.03.031, 2019.

Moecher, D. P., and Samson, S. D.: Differential zircon fertility of source terranes and natural bias in the detrital zircon record: Implications for sedimentary provenance

https://doi.org/10.5194/essd-2026-253
Preprint. Discussion started: 20 April 2026

606 analysis, Earth Planet. Sci. Lett., 247, 252-266,
607 https://doi.org/10.1016/j.epsl.2006.04.035, 2006.
608 Myers, W. B., and Darby, D. A.: A compilation of the silt and clay mineralogy from
609 coastal and shelf regions of the Arctic Ocean, Mar. Geol., 454, 106948,
610 https://doi.org/10.1016/j.margeo.2022.106948, 2022.
611 Naidu, A. S., and Mowatt, T. C.: Sources and dispersial patterns of clay minerals in
612 surface sediments from the continental-shelf areas off Alaska, Geol. Soc. Am.
613 Bull., 94, 841-854, https://doi.org/10.1130/0016-
614 7606(1983)94%3C841:SADPOC%3E2.0.CO;2, 1983.
615 Natali, S. M., Holdren, J. P., Rogers, B. M., Treharne, R., Duffy, P. B., Pomerance, R.,
616 and MacDonald, E.: Permafrost carbon feedbacks threaten global climate goals,
617 Proc. Natl. Acad. Sci. U.S.A., 118, e2100163118,
618 https://doi.org/10.1073/pnas.2100163118, 2021.
619 Parfenov, L. M., Badarch, G., Berzin, N. A., Khanchuk, A. I., Kuzmin, M. I., Nokleberg,
620 W. J., Prokopiev, A. V., Ogasawara, M., and Yan, H.: Summary of Northeast Asia
621 geodynamics and tectonics, Stephan Mueller Spec. Publ. Ser., 4, 11-33,
622 https://doi.org/10.5194/smsps-4-11-2009, 2009.
623 Pease, V., and Coakley, B.: Circum-Arctic Lithosphere Evolution, Geol. Soc. London
624 Spec. Publ., 460, https://doi.org/10.1144/SP460, 2018.
625 Phillips, R. L., and Grantz, A.: Regional variations in provenance and abundance of ice-
626 rafted clasts in Arctic Ocean sediments: implications for the configuration of late
627 Quaternary oceanic and atmospheric circulation in the Arctic, Mar. Geol., 172, 91-
628 115, https://doi.org/10.1016/S0025-3227(00)00101-8, 2001.
629 Puchkov, V. N., and Ivanov, K. S.: Tectonics of the Northern Urals and Western Siberia:
630 General history of development, Geotectonics, 54, 35-53,
631 https://doi.org/10.1134/S0016852120010100, 2020.
632 Rantanen, M., Karpechko, A. Y., Lipponen, A., Nordling, K., Hyvärinen, O.,
633 Ruosteenoja, K., Vihma, T., and Laaksonen, A.: The Arctic has warmed nearly four
634 times faster than the globe since 1979, Commun. Earth Environ., 3, 168,
635 https://doi.org/10.1038/s43247-022-00498-3, 2022.

https://doi.org/10.5194/essd-2026-253
Preprint. Discussion started: 20 April 2026

636 Rino, S., Komiya, T., Windley, B. F., Katayama, I., Motoki, A., and Hirata, T.: Major
637 episodic increases of continental crustal growth determined from zircon ages of
638 river sands; implications for mantle overturns in the Early Precambrian, Phys.
639 Earth Planet. Inter., 146, 369-394, https://doi.org/10.1016/j.pepi.2003.09.024,
640 2004.
641 Rossak, B. T., Kassens, H., Lange, H., Thiede, J.: Clay mineral distribution in surface
642 sediments of the Laptev Sea: Indicator for sediments provinces, dynamics and
643 sources, in: Land-Ocean Systems in the Siberian Arctic: Dynamics and History,
644 edited by: Kassens, H., Bauch, H., Dmitrenko, I., Eicken, H., Hubberten, H. W.,
645 Melles, M., Thiede, J., and Timokhov, L., Springer, Berlin, Heidelberg, Germany,
646 587-600, https://doi.org/10.1007/978-3-642-60134-7_45, 1999.
647 Rusakov, V. Y., Kuz'mina, T. G., and Lukmanov, R. A.: Assessment of the sediment
648 budget of the Kara and Laptev seas, Cont. Shelf Res., 292, 105506,
649 https://doi.org/10.1016/j.csr.2025.105506, 2025.
650 Safonova, I., Maruyama, S., Hirata, T., Kon, Y., and Rino, S.: LA ICP MS U-Pb ages of
651 detrital zircons from Russia largest rivers: Implications for major granitoid events
652 in Eurasia and global episodes of supercontinent formation, J. Geodyn., 50, 134-
653 153, https://doi.org/10.1016/j.jog.2010.02.008, 2010.
654 Saukel, C., Stein, R., Vogt, C., and Shevchenko, V. P.: Clay-mineral and grain-size
655 distributions in surface sediments of the White Sea (Arctic Ocean): indicators of
656 sediment sources and transport processes, Geo-Mar. Lett, 30, 605-616,
657 https://doi.org/10.1007/s00367-010-0210-2, 2010.
658 Schlitzer, R.: Ocean Data View (version 5.6.2) [Software],
659 https://hdl.handle.net/10013/epic.07f8e9e9-6111-47e9-a6dd-494af6f01c7b, 2022.
660 Screen, J. A., and Simmonds, I.: The central role of diminishing sea ice in recent Arctic
661 temperature amplification, Nature, 464, 1334-1337,
662 https://doi.org/10.1038/nature09051, 2010.
663 Serreze, M. C., and Barry, R. G.: Processes and impacts of Arctic amplification: A
664 research synthesis, Glob. Planet. Change, 77, 85-96,
665 https://doi.org/10.1016/j.gloplacha.2011.03.004, 2011.

https://doi.org/10.5194/essd-2026-253
Preprint. Discussion started: 20 April 2026

666 Shi, F., Shi, X., Su, X., Fang, X., Wu, Y., Cheng, Z., and Yao, Z.: Clay minerals in Arctic
667 Kongsfjorden surface sediments and their implications on provenance and
668 paleoenvironmental change, Acta Oceanol. Sin., 37, 29-38,
669 https://doi.org/10.1007/s13131-018-1220-6, 2018.
670 Stein, R., Dittmers, K. , Fahl, K., Kraus, M., Matthiessen, J., Niessen, F., Pirrung, M.,
671 Polyakova, Ye., Schoster, F., Steinke, T., and Fütterer, D.K.: Arctic (Palaeo) River
672 Discharge and Environmental Change: Evidence from Holocene Kara Sea
673 Sedimentary Records, Quat. Sci. Rev., 23, 1485-1511,
674 https://doi.org/10.1016/j.quascirev.2003.12.004, 2004.
675 Stein, R., Frederichs, T., Fahl, K., Geibert, W., and Jansen, E.: A 430 kyr record of ice-
676 sheet dynamics and organic-carbon burial in the central Eurasian Arctic Ocean,
677 Nat. Commun., 16, 3822, https://doi.org/10.1038/s41467-025-59112-7, 2025.
678 Stein, R., Grobe, H., Wahsner, M., 1994. Organic carbon, carbonate, and clay mineral
679 distributions in eastern central Arctic Ocean surface sediments, Mar. Geol., 119,
680 269-285, https://doi.org/10.1016/0025-3227(94)90185-6, 1994.
681 Stein, R., Matthiessen, J., Niessen, F., Krylov, R., Nam, S., and Bazhenova, E.: Towards
682 a better (Litho-) Stratigraphy and Reconstruction of Quaternary Paleoenvironment
683 in the Amerasian Basin (Arctic Ocean), Polarforschung, 79, 97-121,
684 https://epic.awi.de/id/eprint/22435/1/Ste2010b.pdf, 2010.
685 Stein, R.: Arctic Ocean Sediments: Processes, Proxies, and Paleoenvironment, Elsevier,
686 Amsterdam, Netherlands, 1-592, ISBN 9780444520180, 2008.
687 Stein, R.: Clay minerals in Arctic Ocean surface sediments [dataset]. PANGAEA,
688 https://doi.org/10.1594/PANGAEA.992954, 2026a.
689 Stein, R.: Heavy minerals in Arctic Ocean surface sediments [dataset]. PANGAEA,
690 https://doi.org/10.1594/PANGAEA.992955, 2026b.
691 Stevenard, N., Montero-Serrano, J.-C., Eynaud, F., St-Onge, G., Zaragosi, S., and
692 Copland, L.: Lateglacial and Holocene sedimentary dynamics in northwestern
693 Baffin Bay as recorded in sediment cores from Cape Norton Shaw Inlet (Nunavut,
694 Canada), Boreas, 51, 532-552, https://doi.org/10.1111/bor.12575, 2022.
695 Stroeve, J., and Notz, D.: Changing state of Arctic sea ice across all seasons, Environ.

https://doi.org/10.5194/essd-2026-253
Preprint. Discussion started: 20 April 2026

Res. Lett., 15, 103001, https://doi.org/10.1088/1748-9326/aade56, 2018.

Thiry, M.: Palaeoclimatic interpretation of clay minerals in marine deposits: an outlook from the continental origin, Earth Sci. Rev., 49, 201-221, https://doi.org/10.1016/S0012-8252(99)00054-9, 2000.

Timmermans, M.-L., and Marshall, J.: Understanding Arctic Ocean Circulation: A Review of Ocean Dynamics in a Changing Climate, J. Geophys. Res. Oceans, 125, e2018JC014378, https://doi.org/10.1029/2018JC014378, 2020.

Toro, J., Miller, E. L., Prokopiev, A. V., Zhang, X., and Veselovskiy, R.: Mesozoic orogens of the Arctic from Novaya Zemlya to Alaska, J. Geol. Soc., 173, 989-1006, https://doi.org/10.1144/jgs2016-083, 2016.

Troupin, C., Barth, A., Sirjacobs, D., Ouberdous, C. M., Brankart, J.-M., Brasseur, D., Rixen, M., Alvera-Azcárate, A., Belounis, M., Capet, A., Lenartz, F., Toussaint, M.-E., and Beckers, J.-M.: Generation of analysis and consistent error fields using the Data Interpolating Variational Analysis (DIVA), Ocean Model., 52–53, 90–101, https://doi.org/10.1016/j.ocemod.2012.05.002, 2012.

Tütken, T., Eisenhauer, A., Wiegand, B., and Hansen, B. T.: Glacial-interglacial cycles in Sr and Nd isotopic composition of Arctic marine sediments, Mar. Geol., 182, 351-372, https://doi.org/10.1016/S0025-3227(01)00248-1, 2002.

Viscosi-Shirley, C., Mammone, K., Pisias, N. G., and Dymond, J. R.: Clay mineralogy and multi-element chemistry of surface sediments on the Siberian-Arctic shelf: implications for sediment provenance and grain size sorting, Cont. Shelf Res., 23, 1175-1200, https://doi.org/10.1016/S0278-4343(03)00091-8, 2003.

Vogt, C., and Knies, J.: Sediment pathways in the western Barents Sea inferred from clay mineral assemblages in surface sediments, Nor. J. Geol., 89, 41-55, https://doi.org/10.1594/PANGAEA.853649%3E, 2009.

Vogt, C.: Bulk mineralogy in surface sediments from the eastern central Arctic Ocean, Ber. Polarforsch., 212, 159-171, https://hdl.handle.net/10013/epic.10213.d001, 1996.

Vogt, C.: Regional and temporal variations of mineral assemblages in Arctic Ocean sediments as climatic indicator during glacial/interglacial changes, Ph.D. thesis,

https://doi.org/10.5194/essd-2026-253
Preprint. Discussion started: 20 April 2026

726 Fachbereich Geowissenschaften, University of Bremen, Bremerhaven, Germany,
727 309 pp., 1997.
728 Wahsner, M., Müller, C., Stein, R., Ivanov, G. I., Levitan, M. A., Shelekhova, E. S., and
729 Tarasov, G. A.: Clay-mineral distribution in surface sediments of the Eurasian
730 Arctic Ocean and continental margin as indicator for source areas and transport
731 pathways-a synthesis, Boreas, 28, 215-233, https://doi.org/10.1111/j.1502-
732 3885.1999.tb00216.x, 1999.
733 Wang, C. Y., Campbell, I. H., Stepanov, A. S., Allen, C. M., and Burtsev, I. N.: Growth
734 rate of the preserved continental crust: II. Constraints from Hf and O isotopes in
735 detrital zircons from Greater Russian Rivers, Geochimi. Cosmochim. Ac., 75,
736 1308-1345, https://doi.org/10.1016/j.gca.2010.12.010, 2011.
737 Wang, K., Shi, X., Dong, J., Bosin, A. A., Astakhov, A. S., and Yao, Z.: Sediment
738 provenance of the East Siberian Arctic Shelf and evidence of Holocene climate-
739 driven fluvial events in the Indigirka River based on detrital mineral analysis,
740 Palaeogeog. Palaeoclimatol. Palaeoecol., 638, 112042,
741 https://doi.org/10.1016/j.palaeo.2024.112042, 2024.
742 Wang, K., Shi, X., Yao, Z., Bosin, A. A., and Hu, L.: Sediment sources and transport
743 pathways on shelves of the Chukchi and East Siberian Seas: Evidence from the
744 heavy minerals and garnet geochemistry, Polar Sci., 33, 100873,
745 https://doi.org/10.1016/j.polar.2022.100873, 2022.
746 White, D., Hinzman, L., Alessa, L., Cassano, J., Chambers, M., Falkner, K., Francis, J.,
747 Gutowski, W. J., Jr., Holland, M., Holmes, R. M., Huntington, H., Kane, D.,
748 Kliskey, A., Lee, C., McClelland, J., Peterson, B., Rupp, T. S., Straneo, F., Steele,
749 M., Woodgate, R., Yang, D., Yoshikawa, K., and Zhang, T.: The arctic freshwater
750 system: Changes and impacts, J. Geophys. Res. Biogeosci., 112, G04S54,
751 https://doi.org/10.1029/2006JG000353, 2007.
752 White, W. M.: Geochemistry, John Wiley and Sons, Hoboken, NJ, USA, 960 pp., ISBN
753 9780470656679, 2013.
754 Wilson, M. J.: Weathering of the primary rock-forming minerals: processes, products
755 and rates, Clay Miner., 39, 233-266, https://doi.org/10.1180/0009855043930133,

https://doi.org/10.5194/essd-2026-253
Preprint. Discussion started: 20 April 2026

2004.

Xiao, W., Polyak, L., Wang, R., Not, C., Dong, L., Liu, Y., Ma, T., and Zhang, T.: A sedimentary record from the Makarov Basin reveals changing Middle to Late Pleistocene glaciation patterns, Quat. Sci. Rev., 270, 107176, https://doi.org/10.1016/j.quascirev.2021.107176, 2021.

Yao, Z., Feng, H., Stein, R., Liu, Y., Shi, X., Vasilenko, Y., Nam, S.-I., Dong, L., Shi, F., Wang, K., Chen, Z., Qiao, S., Li, Q., Zhao, S., Pei, X., Guo, H., and Liu, Y.: Clay and detrital minerals, Sr-Nd isotopes, and zircon U-Pb ages in Arctic Ocean surface sediments – Circum-Arctic Sediment PROvenance Database (CASPROD): A database of mineralogy and geochemistry for the Circum-Arctic surface sediments, Figshare [dataset], https://doi.org/10.6084/m9.figshare.31926927, 2026.